

Also FERMILAB-PUB-19-085-AD-APC

**Dynamical Simulations of the Muon Campus at Fermilab\***D. A. Tarazona<sup>†</sup>, M. Berz and K. Makino*Department of Physics and Astronomy,  
Michigan State University,  
220 Trowbridge Road  
East Lansing, MI 48824, USA*D. Stratakis, M. J. Syphers<sup>1</sup>*Accelerator Division,  
Fermi National Accelerator Laboratory,  
Pine Street and Kirk Road,  
Batavia, IL, USA*<sup>1</sup>*also at Northern Illinois University, DeKalb, IL, USA*

Received 28 February 2019

Revised 19 June 2019

Accepted 22 June 2019

The Muon Campus at Fermilab is a system through which muons are delivered to the storage ring of the Muon  $g-2$  Experiment (E989). It consists of a set of 1-km beamlines that transport and prepare a highly polarized muon beam out of secondaries produced downstream a target station. Realistic simulations of this beam delivery system (BDS) using *COSY INFINITY*, and presented here, contribute to the understanding and characterization of the muon beam production in relation to the statistical and systematic uncertainties of the E989 measurement, intended to be smaller than 0.14 parts per million to achieve the goals of the experiment. The impact of nonlinearities from fringe fields and high-order contributions on the BDS performance are presented, as well as detailed studies of the interactions between secondaries and the beamline elements apertures, particle decay channels, spin dynamics, and beamline misalignments.

*Keywords:* muon beam; beamlines; simulation; beam performance; nonlinearities; Fermilab; Muon  $g-2$  Experiment; *COSY INFINITY*.

**1. INTRODUCTION**

The most recent measurement of the muon magnetic anomaly,  $a_\mu = (g - 2)/2$ , at the Brookhaven National Laboratory Muon  $g-2$  Experiment (E821) yielded an experimental relative uncertainty of 0.54 ppm, which differs from current Standard Model (SM) predictions by about  $3.7\sigma$ .<sup>1</sup> In contrast to E821, the goal of the Muon  $g-2$  Experiment at Fermilab (E989) is to deliver a measurement of the anomaly to

\*Fermilab report: FERMILAB-PUB-19-085-AD-APC

<sup>†</sup>Email: tarazona@msu.edu. ORCID: 0000-0002-7823-7986.

a precision of 0.14 ppm or less to reach more than  $5\sigma$  discrepancy with the SM and therefore strongly establish evidence for new physics.

For that purpose, the number of recorded high-energy positrons from muon decay in the  $g$ -2 storage ring at E989 is required to increase by a factor of 20 with respect to E821. The Fermilab Muon Campus E989 beam delivery system (BDS), which is a set of 1 km-long beamlines between the pion-production target and the entrance of the Muon  $g$ -2 Storage Ring (SR) downstream, is designed to meet the statistical goal and deliver  $(0.5\text{--}1.0) \times 10^5$  muons to the storage ring per  $10^{12}$  protons that arrive to the pion-production target.

On the other hand, the relative statistical uncertainty in the experimental  $a_\mu$  is inversely proportional to the muon beam polarization (see Eq. 16.6 in Ref. 1). Thus, it is worth to study the effect of nonlinearities and perform spin dynamics simulations. In addition, due to the momentum acceptance of about  $\pm 0.5\%$  of the storage ring, it is of interest to numerically evaluate the dynamical properties of the muon beam as it is delivered to the storage ring.

Motivated by the reasons exposed above, we have developed a model of the E989 beamlines to reproduce numerical simulations of the muon beam's statistical performance and dynamical behavior including spin using *COSY INFINITY*.<sup>2</sup> This program prepares detailed high-order transfer maps calculated with an 8th order Runge-Kutta integrator and Differential-Algebraic (DA) methods to solve the beam optics Ordinary Differential Equations (ODEs) to perform beam tracking. In particular, we present results from tracking of secondary protons, pions, daughter muons from pion decay, and muons produced right at the entrance of the E989 beamlines downstream the pion-production target. Nonlinear effects due to standard fringe fields, up to 4th-order beam dynamics, spin dynamics, beam collimation, and misalignments of the multiple BDS beamline elements are examined.

The paper begins with a brief description of the Muon Campus E989 beam delivery system. Then, details of the beam dynamics simulations throughout the E989 beamlines from the production target to the storage ring entrance and beam performance results modeling nonlinear effects are discussed.

## 2. E989 Beam Delivery System (BDS)

The main purpose of the E989 beamlines analyzed in simulations, depicted in Fig. 1, is to deliver a clean muon beam with momentum  $p_0 = 3.094 \text{ GeV}/c$  to the storage ring. Batches of four bunches made of  $10^{12}$  protons each are directed to an Inconel-600 “pion-production” target located at the AP0 target hall, from which positive secondary particles emerge. A 232 T/m magnetic gradient produced by a lithium lens focuses the secondaries at 30 cm downstream the target. Thereafter, a pulsed magnet with a field of 0.53 T selects  $3.115 \text{ GeV}/c \pm 10\%$  positive particles and bends them  $3^\circ$  towards the 50 m long M2 line, which consists of matching quadrupoles followed by eight more quadrupoles and a dipole that horizontally bends the beam  $3^\circ$  to match with the M3 line (230 m long).

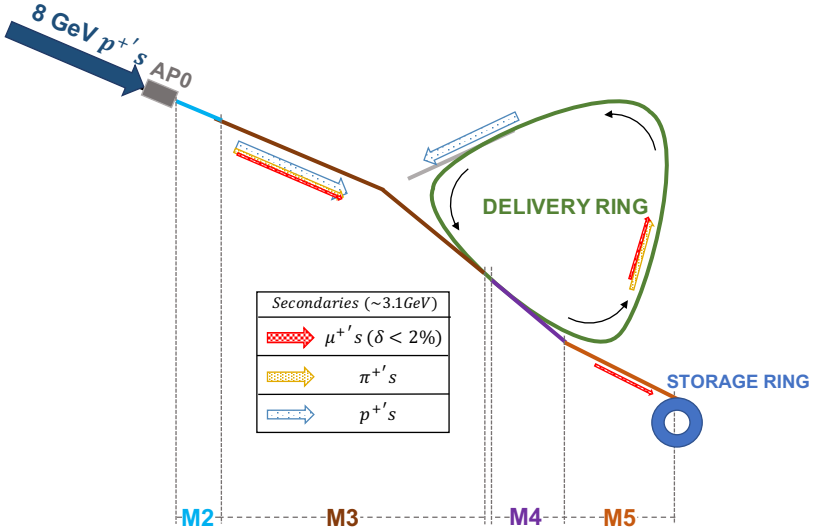


Fig. 1. A schematic layout of the beam delivery system (BDS). Secondary particles (mostly pions, muons, and protons) downstream the target station at AP0 are canalized through the M2/M3 lines and injected to the Delivery Ring (DR) where protons are discarded after four turns. A cleaner beam of mostly muons is extracted to the M4/M5 lines and ultimately delivered to the Muon  $g-2$  Storage Ring (SR).

The M3 line is made of FODO cells that maintain small beta functions to provide continuity of pions and daughter muons from pion decay. By the end of M3, the secondary beam is mainly composed of protons that do not interact with the target, pions that need more time to decay, and muons. In order for such beam to become a clean muon beam, the M3 line is aligned with the injection leg of the Delivery Ring (DR) for which horizontal bends deviate the beam to its horizontal right side by about  $18^\circ$  at  $s \sim 160\text{m}$  away from the target ( $s$  represents the longitudinal distance). At the end of M3, a series of magnets involving a C-magnet, a pulsed magnetic septum dipole, and kicker modules inject the beam DR after a vertically upward bend of about  $5.7^\circ$ .

Through the 505 m of circumference of the DR, previously used as a debuncher ring and now reconditioned for E989, the remaining pions have enough time to decay into mostly muons as they circulate four times before being extracted into the M4 line. The DR also allows protons to spatially separate from the other lighter particles by a rate of 75 ns per turn;<sup>3</sup> this feature lets a kicker within the DR to safely remove the protons after the fourth turn. The optics functions of the DR using *COSY* are shown in Fig. 2.

The resulting muon beam is then extracted to the multiple vertical bends and quads of the M4 beamline (30 m), followed by the M5 line (100 m) with a tunable

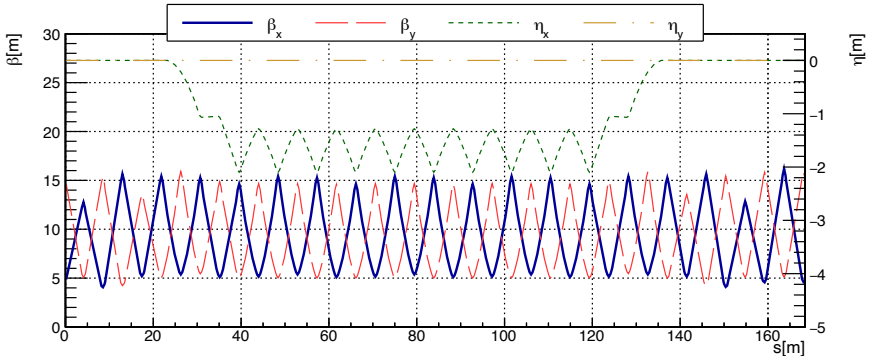


Fig. 2. Optics functions at a three-fold symmetric section of the delivery ring (DR) where the longitudinal distance of the beamline is shown in the horizontal axis. Fringe fields modeled in simulations change the beta functions,  $\beta_x$  and  $\beta_y$ , by less than 3%. Optics functions have served as a channel to validate our BDS model.

final focus section and it is ultimately delivered into the entrance of the storage ring.

### 3. SIMULATION DETAILS AND RESULTS

The following results have served to benchmark other numerical studies at E989<sup>3,4</sup> modeled with *G4beamline*<sup>5</sup> and *Bmad*.<sup>6</sup> Moreover, the inclusion of nonlinearities from fringe fields and high-order effects into our *COSY* model, altogether with an analysis covering various misalignment scenarios, provides further realism to the characterization of the muon beam that is delivered to the storage ring.

Tracking simulations of the E989 beamlines start with a currently available 6D initial distribution at the exit of the pion-production target from a modeling with *MARS*<sup>7</sup> of  $10^9$  protons on target.<sup>8</sup> Work is underway by members of the Muon *g-2* Collaboration to build a *G4beamline* model of the target. We survey the performance of protons, muons, and pions along the BDS in simulations, although other particles emerge from the target as verified by experimental evidence though at significantly smaller ratios.

The presented studies account for aperture beam collimation. There are several aperture geometries determined by the multiple purposes of the elements in the E989 beamlines as well as the expected beam size behavior from design. They range from simple squared and circular apertures to more involved star-shaped apertures which can be approximated as an overlaying of ellipses and rectangles in *COSY*. In simulations, particles are removed from the beam if their spatial transversal coordinates surpass the dimensions of the aperture. This algorithm is repeated approximately every 20 cm depending on the beamline element longitudinal size. *COSY* permits to track arrays of multiple-particle coordinates simultaneously at computational times comparable to the case of single-particle tracking. In this way, the statistical

performance of the beam and resulting beam dynamics variable distributions are computed in a timely manner.

Figure 3 shows the number of secondaries throughout the M2 and M3 lines after the production target. At the end of these lines about  $10^{-4}$  protons per proton on target (POT) remain within the secondary beam, which are kicked out downstream at the Delivery Ring. The in-flight decay channels included in simulations are  $\pi^+ \rightarrow \mu^+ + \nu_\mu$  and  $\mu^+ \rightarrow e^+ + \nu_e + \bar{\nu}_\mu$ . The effect of muon decays on the overall number of muons throughout the beamlines is not significant due to the short time it takes for the beam to travel from the production target to the entrance of the storage ring, i.e.  $8.1 \mu\text{s}$ . Since the momentum admittance at the storage ring is  $\pm 0.5\%$ , we track muons within specific momentum offsets,  $\delta$ , as shown in Fig. 3.

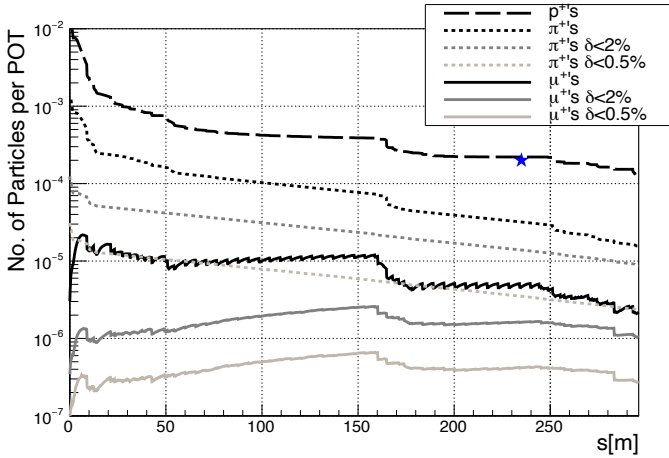


Fig. 3. Statistical performance along M2/M3 lines with the longitudinal distance of the beamline in the horizontal axis. Main muon losses of about 11% and 20% take place at the  $18.5^\circ$  horizontal bend ( $s \sim 160.0\text{ m}$ ) and along the vertical injection upstream the DR ( $s \sim 280.0\text{ m}$ ), respectively. The star-shaped marker around  $s \sim 235\text{ m}$  depicts the number of total particles per POT from measurements (Ref. 9, Fig. 3), suggesting reliability on our simulations results.

The specific range  $|\delta| < 2\%$  is analyzed as well, in connection with upcoming efforts at E989 to manipulate the beam momentum range with wedge cooling.<sup>10</sup> As shown in Fig. 3, M2/M3 lines maintain the statistics of muons with  $|\delta| < 2\%$  emerging from pion decay. Aperture beam collimation allows to predict the final beam momentum distribution at the entrance of the SR, shown in Fig. 4, which is in agreement with results from numerical studies using *G4beamline* (see Ref. 3). Similar simulations were performed along the rest of the E989 beamlines downstream M3 (results are summarized in Table 1).

In addition to the linear description of the beam dynamics, *COSY INFINITY* allows the computation of high-order effects of the beamline elements.<sup>11</sup> In specific,

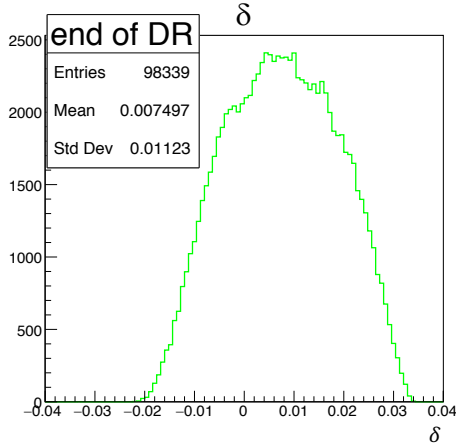


Fig. 4. Beam relative momentum distribution at the storage ring entrance from simulations. One of the main goals of the beam delivery system is to maximize the number of muons with momentum offsets  $|\delta| < 0.5\%$  that are within the momentum acceptance of the storage ring.

Table 1. Statistical performance of protons ( $p$ ), muons ( $\mu$ ), and pions ( $\pi$ ) along the BDS (quantities per POT).

	M3 exit	DR exit ( $n = 4$ )	SR entrance
$\mu$ 's	$2.19 \times 10^{-6}$	$1.04 \times 10^{-6}$	$7.48 \times 10^{-7}$
$\mu$ 's*	$2.72 \times 10^{-7}$	$2.85 \times 10^{-7}$	$1.89 \times 10^{-7}$
$\pi$ 's	$1.55 \times 10^{-5}$	0	0
$p$ 's**	$1.24 \times 10^{-4}$	$6.80 \times 10^{-5}$	$5.86 \times 10^{-5}$

\*Results for  $\delta < 0.5\%$

\*\*Results for the case of proton removal at DR turned off.

particle coordinates as defined in *COSY* are calculated as follows:

$$r_i = \sum_{l_1, l_2, \dots, l_6=0}^{\leq 4} (r_i | x^{l_1} a^{l_2} y^{l_3} b^{l_4} l^{l_5} \delta^{l_6} ) x_0^{l_1} a_0^{l_2} y_0^{l_3} b_0^{l_4} l_0^{l_5} \delta_0^{l_6} \quad (1)$$

where the expression in parenthesis indicates the corresponding transport map component, up to fourth-order in our simulations. As shown in Fig. 5, high-order components seem not to change the statistical performance of the beam.

Fringe fields map computations are performed at the edges of each beamline element. The longitudinal-dependent tapering of the multipole strengths is modeled by a six parameter Enge function:

$$F(z) = \frac{1}{1 + \exp(a_1 + a_2 \cdot (z/D) + \dots + a_6 \cdot (z/D)^5)}, \quad (2)$$

where  $z$  is the distance perpendicular to the effective field boundary and  $D$  is

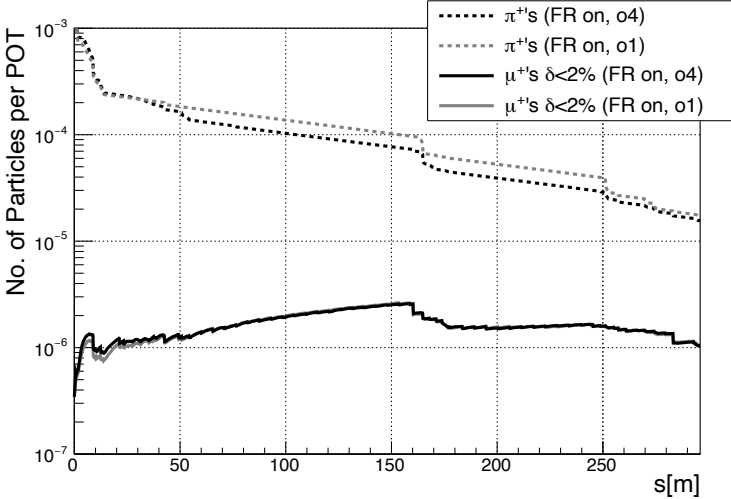


Fig. 5. Simulation results of the number of pions and muons with  $|\delta| < 2\%$  per POT under up to 4th order ( $o4$ ) effects along the M2/M3 lines with fringe fields (FR) turned on. The longitudinal distance along the M2/M3 lines is shown in the horizontal axis. As depicted by the overlapping curves of the muons population for the two  $o1/o4$  cases, linear simulations do not significantly differ from results when high-order terms in the computation of the particle dynamics are simulated.

the full aperture of the particle optical element. The  $a_i$  coefficients are taken by default based on measured data from PEP at SLAC;<sup>11</sup> for such cases, the integrated multipole strengths along the optical axis of each beamline element remain the same as for simulations with hard-edge modeling. Therefore, the following comparisons between numerical results with fringe field effects turned on and off are reliable.

We implemented 4th-order numerical calculations with and without fringe fields. Figure 6 shows the differences between the two scenarios along the DR. After four turns in the DR, simulations suggest a favorable contribution due to fringe fields on the muons (i.e. 9.4% increment) and pions population. Fringe fields introduce fields longitudinal to the beam motion, which may be the essential contributor to keep more particles focused in a similar way to solenoids for low-energy experiments. However, such effect is not sufficiently large to compensate for losses at the beam bends along the beam delivery system in a significant way. In specific, simulation results show an increment of 5.2% more muons at the entrance of the storage ring. Furthermore, fringe fields have a larger contribution in the number of surviving muons than in pions; i.e. at the end of the M3 line ( $s = 290$  m) —where most of pions still have not decayed—fringe fields maintained 8.9% more muons on track whereas pions population at that location increased by only 0.4%, which is within the  $\sim 2\%$  range of the simulations' statistical error.

On the other hand, fringe fields from the BDS beamline elements were also

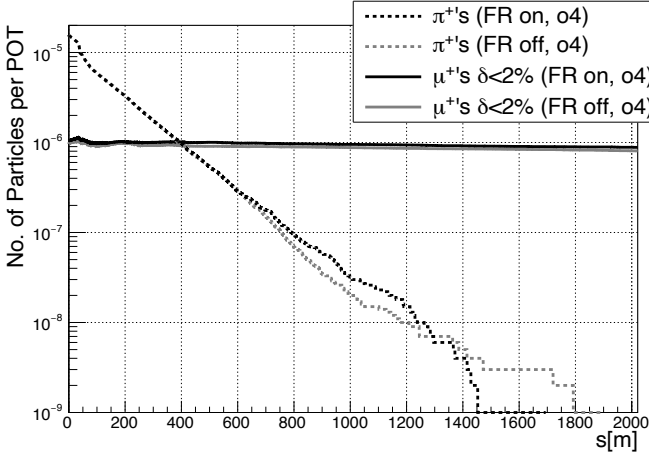


Fig. 6. Fringe field effects on the population of pions and muons along the delivery ring (DR). The horizontal axis represents the longitudinal distance corresponding to four consecutive turns in the DR. From the *COSY*-based BDS model simulations, fringe fields (FR) contribute to maintaining more pions within the apertures of the DR which consequently increase the population of muons by 9.4% before being extracted to the M4 line. The “o4” abbreviation in the legend denotes the order of the computation (i.e. 4-th order).

modeled in spin tracking simulations. For the pion decay channel, the resulting muon beam polarization is calculated based on a module that considers the weak interaction process to get the direction of the muon spin vector,<sup>12</sup> thereafter tracked with *COSY*’s DA mapping calculation.<sup>11</sup>

In Fig. 7, the spin components of a beam made of 64,902 muons at the entrance of the SR are plotted from simulations. The spin components are expressed in terms of the coordinates that describe the relative dynamics around the reference orbit.<sup>13</sup> The resulting polarization is  $P = 0.97$ , in agreement with *G4beamline* numerical simulations<sup>3</sup> which do not include fringe fields. Thus, fringe fields do not interfere with the muon beam polarization. Another spin variable worth to analyze is the angle between the spin vector projection in the horizontal plane and the reference optical axis,  $\varphi_a$ , which resembles the phase that is indirectly measured in the storage ring (see Fig. 8). The muon beam average precession frequency of this phase,  $\langle\omega_a\rangle$ , plays an essential role in the final measurement of  $a_\mu^{E989}$  which implies a deep understanding of its evolution as the beam circulates through the SR. In particular, the correlation between  $\varphi_a$  and the Lorentz factor  $\gamma$  of a muon might result in a sub-ppm systematic effect of  $\langle\omega_a\rangle$ . High-momentum muons decay at a slower rate than low-momentum muons – which might be lost at higher rates, too, before they decay depending on the stored beam matching with the storage ring and nonlinear effects – and as a consequence  $\langle\omega_a\rangle$  could shift as the muon beam decays.<sup>14</sup>

Tracking simulations were performed with and without fringe fields to study the

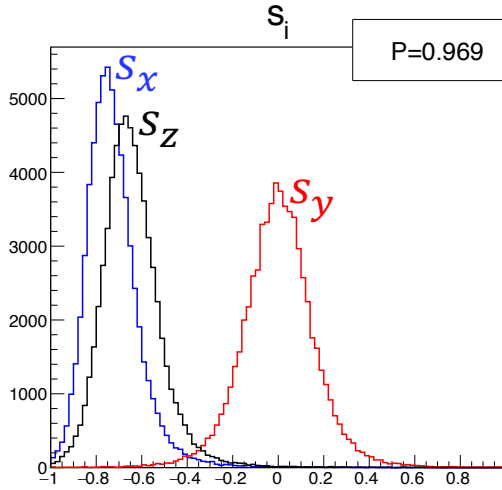


Fig. 7. Histogram of the normalized muon beam spin components (in natural units) at the storage ring entrance from the *COSY*-based BDS model simulations. The high polarization,  $P$ , of the beam is centered with the horizontal plane.

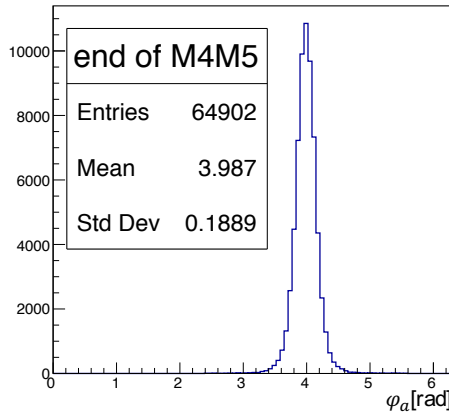


Fig. 8. Histogram of the muons' spin projection angle in the horizontal plane with respect to the reference optical axis at the storage ring (SR) entrance from simulations. The beam delivery system (BDS) is designed to favor the capture of muons from pion decay that are longitudinally polarized. However, as the muon beam travels through the bending sections of the the BDS –especially along the delivery ring which houses multiple rectangular bending magnets– the polarization develops a transversal component while the beam is delivered to the SR.

effect of fringe fields on the spin-momentum correlation  $m_\delta = d\langle\varphi_a\rangle/d\gamma$ . For the case of fringe fields turned on, simulations show a correlation  $m_\delta$  equal to  $29.2 \pm 9.4$  mrad after four turns around the DR as shown in Fig. 9. On the other hand, similar simulations without fringe fields —conventional hard-edge model— indicate a correlation  $m_\delta = 92.1 \pm 9.8$  mrad. This unexpected discrepancy on spin-momentum correlations apparently originated from fringe field effects of the numerous magnetic beamline elements within the DR, specially the rectangular bending magnets, is worthy of more detailed studies. In specific, the large error bars in Fig. 9 can be reduced by increasing the statistics in simulations. Moreover, higher computational orders of the fields that represent the beamline elements in the BDS *COSY*-based ring model could be implemented; in this way, the modeling of fringe fields would encompass higher nonlinear effects.

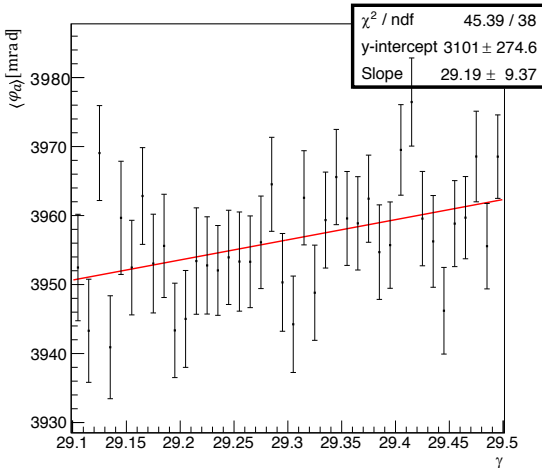


Fig. 9. Beam average of the spin projection angle in the horizontal plane with respect to the reference optical axis,  $\langle\varphi_a\rangle$ , versus the Lorentz factor,  $\gamma$ , at the exit of the delivery ring after four turns. Simulation results presented in this figure correspond to our *COSY*-based BDS model with fringe fields turned on.

Misalignments also studied in our *COSY*-based BDS simulations are introduced by transforming the transport maps that represent each beamline element. Transformations follow randomly Gaussian-distributed horizontal and vertical misplacements with standard deviations of 0.25 mm, introducing constant terms to the maps. A total of ten random misalignment configurations of the beam delivery system initialized with different random seeds were analyzed to procure statistical ranges within which the beam performance would be expected to occupy.

Figure 10 shows how the repercussions of misalignments under consideration

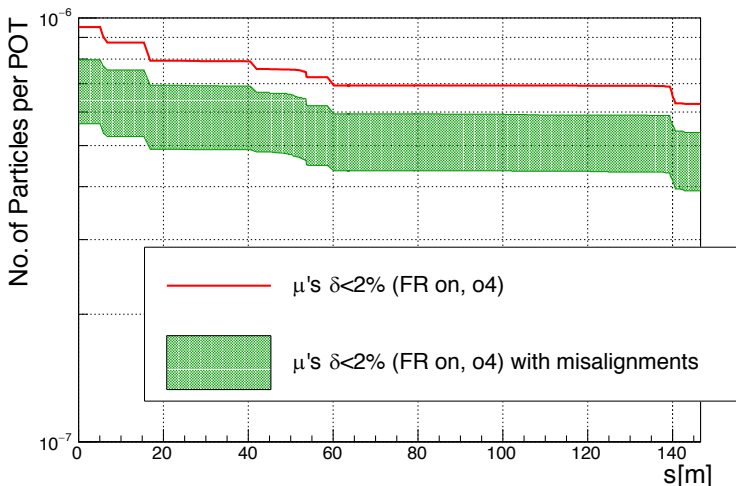


Fig. 10. Simulation results of the muons population with  $|\delta| < 2\%$  under the effects of beamline misalignments along the M4/M5 lines. The number of muons per proton on target (POT) is shown in the vertical axis as a function of the longitudinal distance along the M4/M5 lines. The red line depicts the number of muons for the ideal case of no misalignments present in the beam delivery system. The green band summarizes simulation results for several scenarios of beamline elements randomly misaligned in both vertical and horizontal directions.

could accumulate as muons travel along the BDS, decreasing the number of muons that make it to the end of M5. However, even though 0.25 mm is a small root mean square of the overall misplacements, the correctors along the beamlines are expected to mitigate such detrimental effect.

#### 4. CONCLUSION

A detailed model of the beam delivery system at E989 has been developed using *COSY INFINITY*. Realistic features based on DA methods, such as fringe fields, high-order effects, and misalignments are included to describe the statistical and dynamical performance of the secondary beam produced at the pion-production target. Simulation results suggest that fringe fields increase the number of muons that are delivered to the storage ring by  $\sim 5\%$ , whereas the muon beam polarization is unaffected. However, spin-momentum correlations that could add systematic effects to the final measurement of E989 due to differential decays are significantly affected by the fringe fields from the rectangular dipole magnets of the delivery ring; further studies with higher statistics and computational orders in simulations are pertinent to confirm this effect. Regarding high-order effects, our numerical studies indicate that they do not affect the secondary beam performance along the BDS. In addition to the presented results, the *COSY*-based model served to validate nu-

merical calculations prepared by other members of the Muon  $g-2$  Collaboration and check the performance of the Fermilab Muon Campus E989 beam delivery system.

## ACKNOWLEDGEMENTS

We are thankful to the Muon  $g-2$  Collaboration at Fermilab, specially W.M. Morse, J.P. Morgan, M. Korostelev, and V. Tishchenko for all the discussions and suggestions. In particular, the authors thank V. Tishchenko for providing the initial beam distribution files downstream the target station. This work was supported by the U.S. Department of Energy under Contract No. DE-FG02-08ER41546. This manuscript has been authored by Fermi Research Alliance, LLC under Contract No. DE-AC02-07CH11359 with the U.S. Department of Energy, Office of Science, Office of High Energy Physics. We are grateful to the PhD Accelerator Program at Fermilab and also for a Strategic Partnership Grant from the MSU Foundation.

## References

1. J. Grange *et al.* [Muon  $g-2$  Collaboration at Fermilab], “Muon  $g-2$  Technical Design Report”, Fermi National Accelerator Laboratory, Batavia, IL, USA, FERMILAB-FN-0992-E, Jan. 2015.
2. K. Makino and M. Berz, “COSY INFINITY Version 9”, *Nucl. Instr. Meth. A*, vol. 558, pp. 346–350, 2006.
3. D. Stratakis *et al.*, “Accelerator performance analysis of the Fermilab muon campus”, *Phys. Rev. Accel. Beams*, vol. 20, pp. 111003, Nov 2017.
4. M. Korostelev *et al.*, “End-to-end beam simulations for the new Muon  $g-2$  Experiment at Fermilab,” *Proc. 7th Int. Particle Accelerator Conf. (IPAC’16)*, Busan, Korea, May 2016, paper WEPMW001, pp. 2408–2411.
5. *G4beamline*, <http://www.muonsinternal.com/muons3/G4beamline>.
6. *Bmad*, <https://www.classe.cornell.edu/bmad/>.
7. *MARS*, <http://mars.fnal.gov>.
8. Data provided by the Muon  $g-2$  Collaboration at Fermilab.
9. D. Stratakis *et al.*, “Commissioning and first results of the Fermilab Muon Campus”, *Phys. Rev. Accel. Beams*, vol. 22, pp. 011001, January 2019.
10. J. Bradley *et al.*, “Initial Studies into Longitudinal Ionization Cooling for the Muon  $g-2$  Experiment,” *Proc. 9th Int. Particle Accelerator Conf. (IPAC’18)*, Vancouver, Canada, May 2018, paper TUPMK015, pp. 1522–1525.
11. M. Berz and K. Makino, “COSY INFINITY 10.0 Beam Physics Manual”, Department of Physics and Astronomy, Michigan State University, East Lansing, MI, USA, Rep. MSUHEP-151103, Oct 2017.
12. F. Combley and E. Picasso, The muon ( $g-2$ ) precession experiments: Past, present and future, *Phys. Rep.* 14, 1 (1974).
13. M. Berz, K. Makino, and W. Wan, *An Introduction to Beam Physics*, CRC Press, Boca Raton, FL, USA 2016.
14. J. Crnkovic *et al.*, “Spin Correlations study for the new  $g-2$  Experiment at Fermilab,” *Proc. 7th Int. Particle Accelerator Conf. (IPAC’16)*, Busan, Korea, May 2016, paper TUPMR028, pp. 1301–1303.